

Xu Wang<sup>1</sup>, Xuhao Peng<sup>1</sup>, Haolin Liu<sup>1</sup>, Jiaqing Kou<sup>1</sup> & Weiwei Zhang<sup>1</sup>

<sup>1</sup>School of Aeronautics, Northwestern Polytechnical University, Xi'an, 710072, China

#### **Abstract**

Flutter prediction is an important phenomenon that need to be considered in aircraft design. However, high-fidelity predictions for transonic flutter are difficult to make due to the associated computational costs. This paper proposed a multi-fidelity reduced-order modelling framework for flutter predictions to achieve high-fidelity predictions with less computational costs. Here, the high-fidelity data is obtained from a Navier–Stokes-equation-based solver, while the low-fidelity solution is taken from an Euler-equation-based flow solver. Using the multi-fidelity neural network trained based on the multi-fidelity data, this approach can achieve online predictions of high-fidelity results. To demonstrate the multi-fidelity process, a widely used pitching and plunging airfoil case is considered. Verification of the approach is done by comparing with results from the time-domain aeroelastic solvers. The results show that the proposed multi-fidelity neural network modelling framework can realize the online predictions of unsteady aerodynamic forces and flutter results across multiple Mach numbers. Compared with the typical Co-kriging method, the proposed method has higher accuracy and stronger generalization capability. Finally, the method's potential for reducing the computational effort of high-fidelity aeroelastic analyses is demonstrated.

Keywords: Multi-fidelity; Deep learning; Flutter; Aerodynamics

## 1. Introduction

Flight safety is an important issue that has attracted much attention in the design of large commercial transport aircraft. The push for more efficient transport aircraft leads to larger wingspans and more flexible wing configurations, for which flutter becomes a significant design consideration [1]. Flutter occurs when there is a net gain of energy from a fluid to a structure's modes of vibration, causing a diverging aeroelastic response [2]. A time-domain simulation that couples a computational fluid dynamics (CFD) solver with a computational structural dynamics (CSD) solver can generate the complete aeroelastic response of a structure with nonlinear aerodynamics [3]. However, incorporating flutter prediction into early-stage design is a considerable challenge for the transonic flow regime relevant to most civil transport aircraft designs. Existing accurate models for transonic flutter prediction typically require extensive CFD analyses that are too expensive to conduct in early design stages, where potentially thousands of wing designs might be considered. At the same time, it is difficult to obtain sufficient flutter simulation data for the parameter ranges of concern. There is an increasing need to develop unsteady aeroelastic models for flutter predictions across multiple flow parameters.

To model the unstable aerodynamics more efficiently, aerodynamic reduced-order modeling (ROM) methods [4],[5],[6],[7] have been extensively studied.

As reviewed by Brunton et al. [8], data science and machine learning are rapidly transforming the scientific and industrial landscapes. Recently, with the development of machine learning and data science, data-driven modeling has played an important role in nonlinear unsteady aerodynamic modeling. Due to strong flow separation, viscous effects, and vortex shedding, unsteady aerodynamics

show strong nonlinear behavior [9] under transonic flow. Hence, kriging models [10],[11], higherorder spectra [12], the support vector machine (SVM) method [13], the nonlinear Volterra method [14], and neural networks [15],[16],[17] have been introduced to enhance the nonlinear aerodynamic prediction capabilities. Due to the self-learning, self-adaptive, and fault-tolerance characteristics of neural networks, a series of models based on neural networks have been used to construct nonlinear reduced-order models. Li et al. [18] established an unsteady aerodynamics model for airfoil pitching and plunging in the transonic flow across multiple Mach numbers. It was demonstrated that the model could accurately capture the dynamic characteristics of aerodynamic and aeroelastic systems with varying flow and structural parameters. Zahn et al. [16] proposed a ROM framework based on a long short-term memory (LSTM) neural network for the prediction of transonic buffet aerodynamics, which was favorable for capturing the time-delayed effects associated with unsteady aerodynamics. Winter et al. [19] proposed a fuzzy neural system to predict unsteady aerodynamic loads and flutter boundaries across various freestream conditions. Although a large body of literature has been devoted to applying machine learning techniques in the fluid mechanics field, the gaps and issues left by data-driven surrogate models are still an open issue, compromising their reliable and widespread use in practical applications.

Despite previous efforts in nonlinear aerodynamic system identification resulting in successful practices, there are still challenges impeding the robustness of transonic flutter predictions. Identification of a nonlinear system, which is required to capture large-amplitude motions, varying flow conditions, or separated flows, still remains a challenging task [16]. High-fidelity (HF) reduced-order models require a large amount of data support to provide generalization capabilities across various freestream conditions. In addition, relatively inexpensive approximate aeroelastic models (low-fidelity models) exist and are routinely applied to reduce the cost of estimating flutter, albeit with lower accuracy [20]. Under this condition, it is particularly important to utilize low-fidelity (LF) simulations to reduce the data requirements of high-fidelity reduced-order models and maintain the original simulation accuracy.

In recent years, multi-fidelity (MF) models have been proposed to reduce the amount of data required to obtain a reasonable model through the use of models with different fidelity levels [21],[22]. Multi-fidelity methods have a rich history of application in different areas of science and engineering [23],[24]. Since high-fidelity models are accurate but expensive, while low-fidelity models are inexpensive but less accurate, multi-fidelity methods combine these two types of models to achieve an accurate representation of high-fidelity results at a reasonable cost [25]. The general idea is to combine trends from inexpensive lower-fidelity data (e.g., coarser meshes, low-fidelity computations, and less-sophisticated models) with interpolations of high-fidelity data (e.g., finer meshes, high-fidelity computations, better models, and experimental data) [26]. Based on a co-kriging model [27], Kaya et al. [28] presented a multi-fidelity aerodynamic modeling approach for the aerodynamic database. Recently, a multi-fidelity formulation proposed by Kou and Zhang [29] was developed. They adopted a multi-kernel neural network model to construct a variable-fidelity dynamic model for unsteady aerodynamics. This method combined data from an Euler simulation and a full Navier-Stokes simulation, and it predicted the high-fidelity aerodynamic loads only from three typical harmonic motions with a high level of accuracy. Liu et al.[30] established a transonic buffeting nonlinear aeroelastic fusion model using the limit cycle state harmonic signal. The model built a mapping from low-fidelity moments to high-fidelity moments through data fusion methods. The fusion model coupled the structural motion equation and accurately reproduced the amplitude characteristics of limit-cycle oscillations in the wide frequency range of the frequency-locking region. These works motivated our research on developing multi-fidelity unsteady aerodynamic models for transonic flutter predictions.

This paper presents a multi-fidelity reduced-order modeling (MFROM) method for modeling unsteady aerodynamics, and it investigates both the reductions in the computational expense and the ability of the method to predict the onset of flutter. Based on the proposed neural network architecture, the multi-fidelity model achieves online prediction of the lift and moment coefficients across multiple Mach numbers. The flutter prediction results for the NACA64A010 airfoil showed that the MFROM model can balance the accuracy and efficiency of the prediction. Modeling results of the MFROM validated the generalization capability for different Mach number, angle of attacks, and reduced frequencies.

# 2. Comparison of multi-fidelity aerodynamics

To establish the multi-fidelity aerodynamics model, two types of CFD simulation results were considered. Unsteady Euler-equation-based computations and unsteady Navier–Stokes-equation-based computations were used for the modeling process. As mentioned above, there is a significant difference in accuracy and efficiency between these numerical simulations. For simplicity of description, these simulations will subsequently be referred to as high-fidelity simulations and low-fidelity simulations. This section presented the NACA64A010 airfoil, which was used in the validation cases. This airfoil is widely used for algorithm validation in the field of aeroelasticity.

The unsteady aerodynamic data were obtained from an unsteady Reynolds-averaged Navier–Stokes (URANS) solver, which solved the URANS equations, and an Euler-equation-based solver, which solved the unsteady Euler equations. The Navier–Stokes and Euler equations are shown, respectively, as follows:

$$\frac{\partial Q}{\partial t} + \frac{\partial (F - F_v)}{\partial x} + \frac{\partial (G - G_v)}{\partial y} + \frac{\partial (H - H_v)}{\partial z} = 0, \tag{1}$$

$$\frac{\partial Q}{\partial t} + \frac{\partial F}{\partial x} + \frac{\partial G}{\partial y} + \frac{\partial H}{\partial z} = 0.$$
 (2)

Where  $Q = [\rho, \rho u, \rho v, \rho w, E]$  denotes the conservation vector, [F, G, H] is the inviscid flux and  $[F_v, G_v, H_v]$  represents the viscous flux. In conservation vector,  $\rho$  represents the density of the fluid, u is the x-direction velocity, v is the y-direction velocity, v is the y-direction velocity, v is the v-direction velocity, and v represents the total internal energy per unit mass of fluid. The Spalart–Allmaras turbulence model [31] was selected to close the Navier–Stokes equations and describe the turbulence fluctuations. The unsteady CFD solver allowed moving bodies through the use of an arbitrary Lagrangian–Eulerian formulation, and the dynamically deforming mesh algorithm was based on radial basis function (RBF) interpolation [32]. To accelerate the convergence of the time-marching, local-time stepping, residual smoothing, and multiple grids were employed. The Euler equations form a simplified version of the flow model, which can be solved relatively efficiently under conditions where viscous effects are not strong.

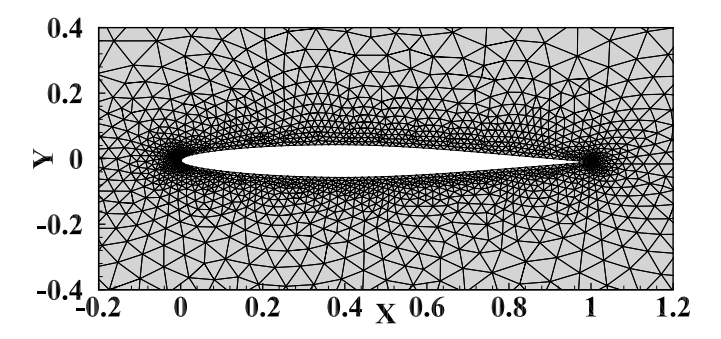


Figure 1 – Grid for low-fidelity (LF) simulations with 4435 cells

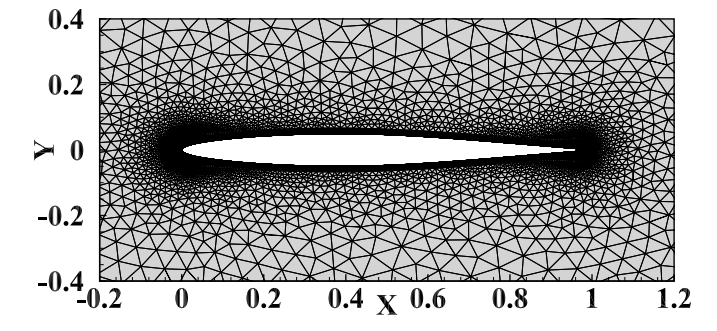


Figure 2 – Grid for high-fidelity (HF) simulations with 18197 cells

The hybrid computational meshes of the NACA64A010 airfoil were used to obtain the unsteady aerodynamic data. The y+ number was less than 1.3 in most of the regions, and the distance between the airfoil and the circular far field was 20c. Fig. 1 shows the computational meshes of the airfoil in detail. To better capture the viscous flow, more cells were used for the HF simulations.

Davis et al. [33] provided wind tunnel test data for the pitching motion of the NACA64A010 airfoil at a Mach number of 0.796, which is a commonly used test case for transonic flow. The reduced frequency  $k = \omega * b/V_{\infty}$  of the pitching motion was 0.202, the mean incidence was 0 deg, and the pitching amplitude was 1.01 deg. The unsteady history of the angles of attack of the airfoil can be expressed as follows:

$$\alpha(t) = \alpha_M \sin(\omega t) + \alpha_0. \tag{3}$$

 $\alpha_M$  represents the amplitude of the pitching motion, and  $\alpha_0$  represents the balanced angle of attack. As shown in Fig. 2, the aerodynamic forces obtained by both types of methods were in better agreement with the experimental results at small angles of attack. All the results were obtained using 16 Intel i7-10700 CPU processors at 2.4 GHz.

These results validated the solver employed and also allowed the accuracy and efficiency to be examined. Due to the consistency of the demonstrated multi-fidelity aerodynamic data, most of the aeroelasticity problems have been solved using numerical simulations based on the Euler equations. This is because high-fidelity methods require more than four times the computational cost of low-fidelity methods. With approximate accuracy, it is clearly more cost-effective to use a low-fidelity model. However, under some conditions, as the difference in accuracy between the two types of methods increases, the difference in the flutter prediction results becomes unacceptable.

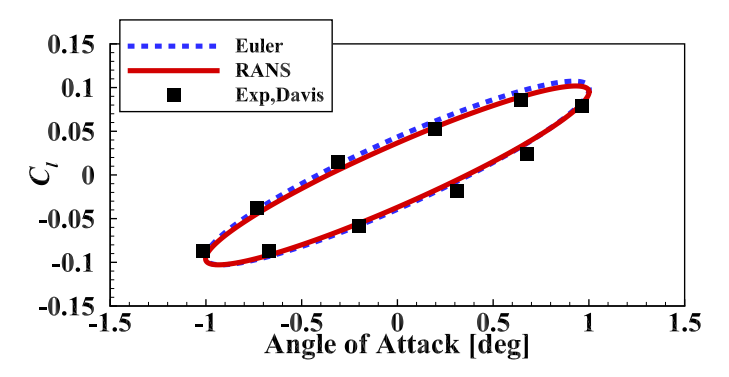


Figure 3 – Comparison of simulation results for  $C_l$  and experimental results

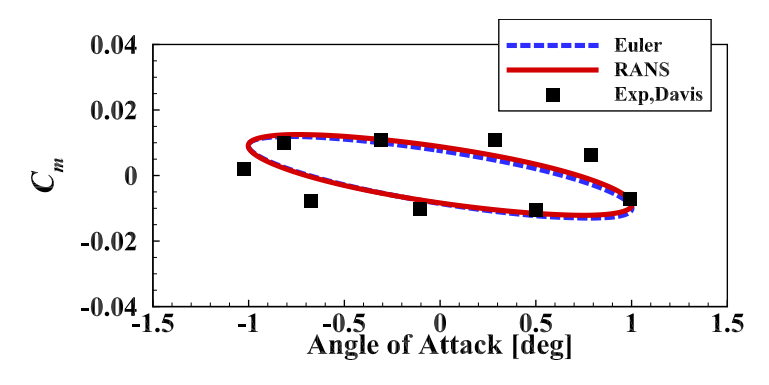


Figure 4 – Comparison of simulation results for  $C_m$  and experimental results

In unsteady simulations with two degrees of freedom, the differences between the solvers are even more unacceptable, resulting in errors in the flutter predictions. This will be analyzed in detail in Section IV. In this case, transonic flutter prediction requires further consideration of the trade-off between accuracy and efficiency. This is the context in which the work in this paper was carried out. We sought to build a data-driven multi-fidelity model with strong generalization capabilities to bridge the gap between high- and low-fidelity data. This makes it possible to obtain predictions with little

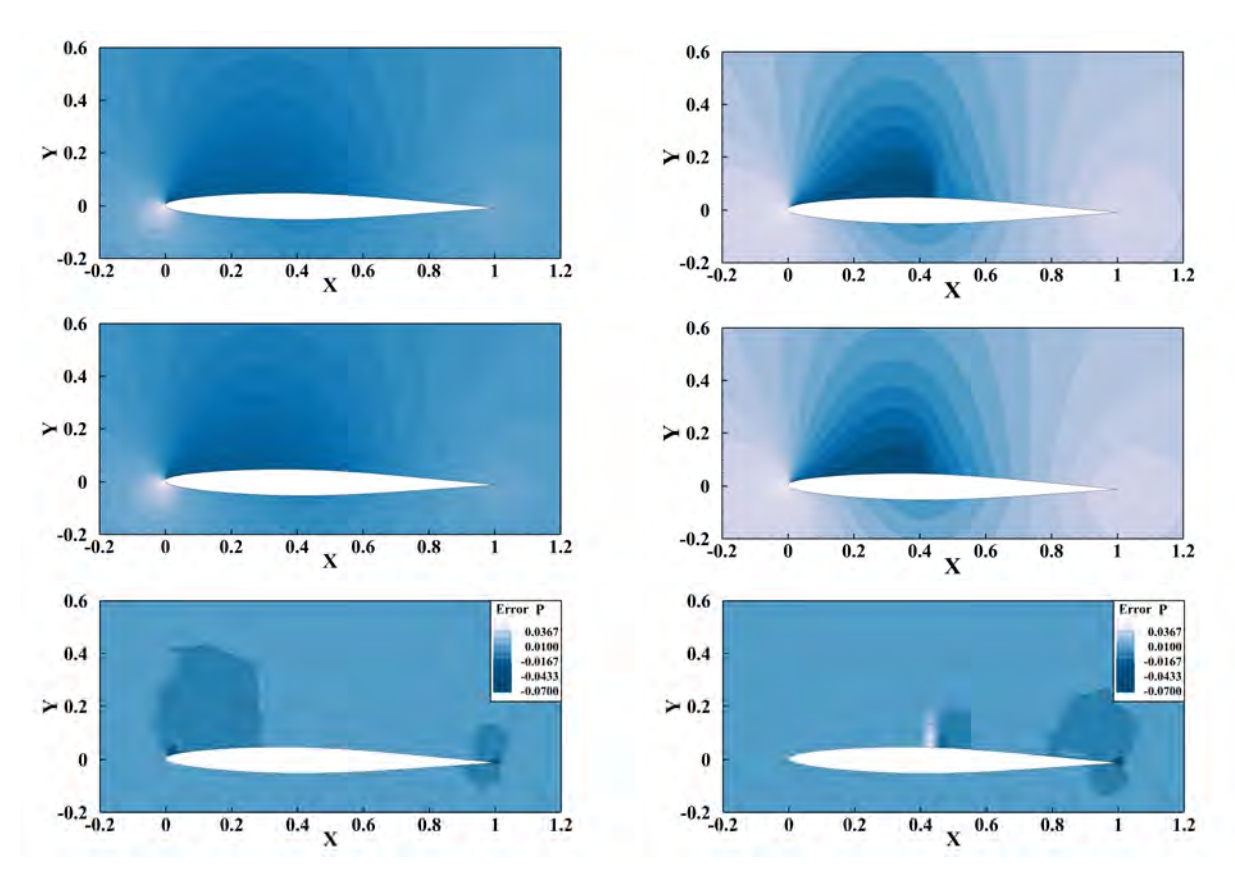


Figure 5 – Comparison of pressure distribution in flow fields with multi-fidelity flow solve

loss of accuracy (compared with the HF results) at little additional cost to the computation (compared with the LF results).

# 3. Multi-Fidelity Reduced-Order Modeling

A multi-fidelity model mainly constructs a relationship between LF and HF data. These models are often used for offline predictions to reduce the sampling costs. However, unsteady aerodynamic modeling is more demanding for the multi-fidelity model. First, the sampling space of the unsteady aerodynamics is much more high-dimensional. Offline prediction methods are not capable of meeting the accuracy requirements of flutter prediction. Second, the nonlinearities of transonic aerodynamics require models with stronger generalization capabilities. These make it difficult to apply existing multifidelity modeling methods to transonic flutter prediction. To avoid the above problems, this paper proposes a multi-fidelity ROM method based on neural networks for online prediction. The method constructs mappings between the offline LF and HF data through neural network training. This neural network can be applied for online aerodynamic predictions and aeroelastic coupling simulations.

## 3.1 Proposed multi-fidelity reduced-order modeling (MFROM) method

The proposed multi-fidelity simulation method for aeroelasticity is shown in Fig. 6. The superscripts L and H here represent LF and HF, respectively. The construction and application of the MFNN-ROM can be divided into two parts: an offline phase and an online phase. In the offline phase, unsteady aerodynamic data with the two methods are obtained by simulations of forced motions. On this basis, the MFNN-ROM is trained through the input and output relationships shown in Fig. 6. In the online phase, LF CFD/CSD coupling simulations are used to generate input data. Here, the predictions of the MFNN-ROM are carried out during the process of time stepping. This is completely different from traditional reduced-order models. Through the design of online prediction, the demand for data in the offline phase can be reduced while ensuring the accuracy of the online simulations.

In the simulation of aeroelasticity, the available inputs for MF modeling include unsteady motions (Inputs-1) and LF aerodynamic forces (Inputs-2). We proposed an MF neural network architecture,

# MTL framework for multi-fidelity aerodynamic prediction

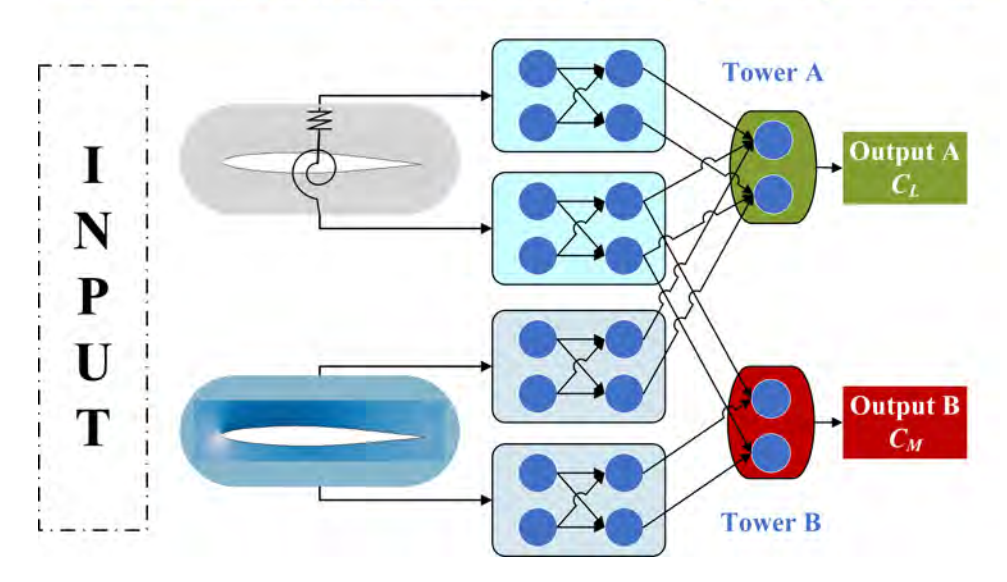


Figure 6 – Proposed MFNN-ROM for aeroelastic flutter prediction

as shown in Fig. 7, to achieve aerodynamic modeling. The model adopts a deep neural network to implement the mapping process.

To reflect the time-delayed effects of unsteady aerodynamics, Zhang [34] proposed to use autoregressive models for modeling unsteady aerodynamics, through the introduction of input and output feedback. This dynamic process is regarded as a nonlinear autoregressive exogenous (NARX) [35] model representation in system identification, composed of a time-delayed input and output feedback. Therefore, the input data are expressed as follows:

$$C_l^{\mathrm{H}}, C_m^{\mathrm{H}} = f[\alpha, h/b, C_l^{\mathrm{L}}, C_m^{\mathrm{L}}], \tag{4}$$

$$C_l^{\rm H}, C_m^{\rm H} = f[\alpha(k)..., \alpha(k-n), h/b(k)..., h/b(k-n), C_l^{\rm L}(k)..., C_l^{\rm L}(k-n), C_m^{\rm L}(k)..., C_m^{\rm L}(k-n)]. \tag{5}$$

As shown in Fig. 7, the proposed multi-fidelity neural network (MFNN) consists of two modules. The blue module represents the mapping parts of the lift and moment coefficients obtained by the LF simulation method. The gray part represents the mapping parts of the unsteady motions. The fully connected module contains 100 neurons total with two layers for mapping. The activation functions are RBFs:

$$g(r^2) = \exp(-\frac{r^2}{2\sigma^2}),$$
 (6)

$$r = |x - c|, (7)$$

where r is the difference between the input of neuron x and neural center c, which is expressed as |x-c|. The deep neural network is connected as shown in Fig. 7. The numbers of neurons in the four hidden layers are [200, 200, 100, 100]. Using the training of these hyperparameters, the model can realize complex mapping relationships between different fidelity data.

To avoid the imbalance of the data size for different losses, the dynamic weight averaging method is selected as the optimization criterion. This method is used to balance the optimization process between multiple losses to ensure consistency. The dynamic weight  $\omega_k(t)$  is calculated as the descending rate by calculating the loss ratio of two adjacent time steps. Therefore, the smaller the weight, the greater the convergence rate, and the simpler the task becomes. This method ensures the balance between multiple losses in the parameter learning process. The loss functions are shown as follows:

$$Loss(t) = \sum_{k} \omega_k(t) L_k(t), \omega_k(t) = \frac{L_k(t-1)}{L_k(t-2)}.$$
 (8)

The error of  $C_i^H$  and  $C_m^H$  is expressed as a relative error, as follows:

$$L_{k} = \sqrt{\frac{1}{N} \sum_{i=1}^{N} \left( C^{i} - C_{pre}^{i} \right)^{2}} / \sqrt{\frac{1}{N} \sum_{i=1}^{N} \left( C^{i} \right)^{2}}.$$
 (9)

For an aeroelastic simulation, the accuracy of the lift and moment coefficients are equally important, and this dynamic weight averaging method can further improve the prediction accuracy of the MF model.

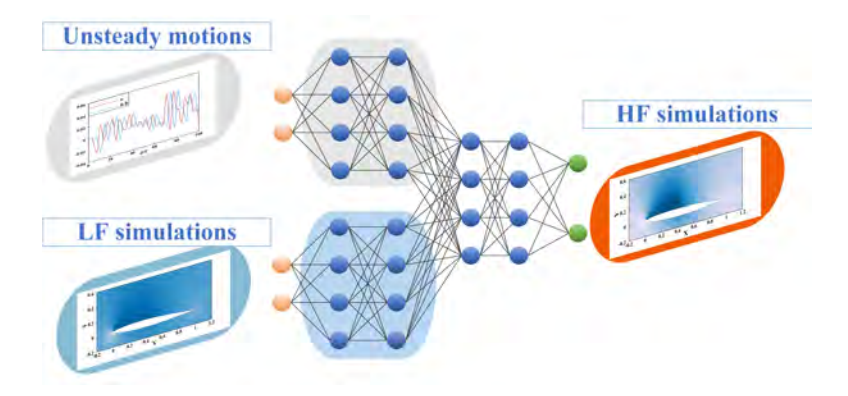


Figure 7 – Multi-fidelity (MF) neural network architecture for multi-fidelity data modeling

For each unsteady case, 100–1000 input–output pairs should be included to provide model training. The model training and hyperparameter optimization are achieved by Particle Swarm Optimization (PSO). PSO algorithm is an optimization algorithm proposed by Kennedy and Eberhart [36] in 1995. The inertia weights are updated through Eq. 12, the  $\omega_1=0.7$  and  $\omega_2=0.9$  are the lower and upper bounds of the weights, and G=100 represents the number of iterations. The particle position is updated through the following equation until the iteration stops, allowing the global optimal solution to be obtained:

$$\mathbf{V}_{i}^{d+1} = \omega(t) \times \mathbf{V}_{i}^{d} + c_{1}r_{1} \times (\mathbf{P}_{i}^{d} - \mathbf{X}_{i}^{d}) + c_{2}r_{2} \times (\mathbf{Gbest}_{i}^{d} - \mathbf{X}_{i}^{d}), \tag{10}$$

$$\mathbf{X}_i^{d+1} = \mathbf{X}_i^d + \mathbf{V}_i^{d+1},\tag{11}$$

$$\omega(t) = \omega_2 - (\omega_2 - \omega_1) \times d/G. \tag{12}$$

For the data volume of this study, the parameter training time of the model was about 30 min, and the time of each prediction calculation example was less than 1 s.

# 3.2 Aerodynamic prediction results and validation

In this section, the tests for the MFNN-ROM in predicting aerodynamic forces across multiple Mach numbers are described. The proposed model can establish the transformation relationship between the MF data. The capability of the model in offline prediction is similar to that of traditional MF models. As a typical MF model, the co-kriging model was used as a comparison to demonstrate the advantages of the proposed model.

Similar to the form of the kriging model, the co-kriging model can be written in the following form:

$$\hat{y}(\mathbf{x}) = \mathbf{f}(\mathbf{x})^T \boldsymbol{\beta} + \mathbf{r}^T (\mathbf{x}) \mathbf{R}^{-1} (\mathbf{y} - \mathbf{F}^T \boldsymbol{\beta}), \tag{13}$$

$$\mathbf{r}(\mathbf{x}) = \left(\rho \cdot \sigma_l^2 \cdot \mathbf{r}_l^T(\mathbf{x}), \rho^2 \cdot \sigma_l^2 \cdot \mathbf{r}_l^T(\mathbf{x}, \mathbf{X}^L) + \sigma_h^2 \cdot \mathbf{r}_h^T(\mathbf{x}, \mathbf{X}^H)\right)^T.$$
(14)

The correlation matrix of the co-kriging model considers the cross-correlation between the LF cases  $X^L$  and the HF cases  $X^H$ :

$$\mathbf{R} = \begin{pmatrix} \sigma_l^2 \cdot \mathbf{R}_l(\mathbf{X}^L, \mathbf{X}^L) & \rho \cdot \sigma_l^2 \cdot \mathbf{R}_l\left(\mathbf{X}^L, \mathbf{X}^H\right) \\ \rho \cdot \sigma_l^2 \cdot \mathbf{R}_l\left(\mathbf{X}^H, \mathbf{X}^L\right) & \rho^2 \cdot \sigma_l^2 \cdot \mathbf{R}_l\left(\mathbf{X}^H, \mathbf{X}^H\right) + \sigma_h^2 \cdot \mathbf{R}_h(\mathbf{X}^H, \mathbf{X}^H) \end{pmatrix}. \tag{15}$$

After optimization of the hyperparameters, the co-kriging model can also be used for unsteady aerodynamic prediction [37].

For validation, the same MF data were used to construct both MF models. The training cases involved harmonic pitching motions at Mach numbers of 0.7 and 0.75. Test cases were obtained by Latin hypercube sampling (LHS). The test cases included different reduced frequencies, balanced angles of attack, and Mach numbers to fully test the generalization capability of the model. The distribution of the cases in the parameter space is shown in Fig. 8.

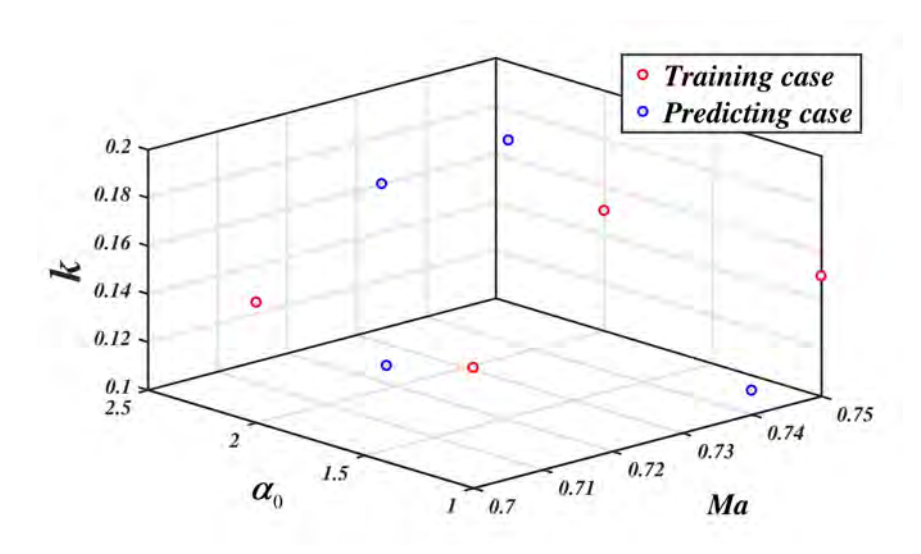


Figure 8 – Distribution of the cases for training and predicting

Table 1 –	Parameters	of training	and p	oredicting	cases

		Trainin	g cases	5		Predictir	ng cases	}
k	0.15	0.15	0.15	0.15	0.11	0.14 1.40 0.702	0.18	0.20
$\alpha_0$	1	1	2	2	1.00	1.40	2.05	1.80
Ma	0.7	0.75	0.7	0.75	0.741	0.702	0.720	0.731

The modeling comparisons for the four test cases are shown in Fig. 9 and 10. The relative errors calculated by Eq. 9 of the prediction cases are shown in Table 2. In the predictions of the lift coefficients, the performances of these two methods were quite close. The predictions of these models agreed very well with the HF results, with a maximum relative error of not more than 2%. The difference was that, in the prediction of moment coefficients, the co-kriging model was limited in accuracy. The co-kriging model exhibited under-correction and over-correction because the trends were no longer consistent between the HF and LF data. By contrast, the prediction accuracy of the MFNN-ROM remained reliable. The relative errors of the prediction results of the neural network model remained below 7%. Compared with classical MF models, the MFNN-ROM had the ability to model unsteady aerodynamics across multiple Mach numbers, with improvements in accuracy. Aeroelastic simulations require modeling capabilities for both lift and moment coefficients. In this case, the MFNN-ROM was clearly a better choice.

Table 2 – Parameters of training and predicting cases

		(	Z <sub>l</sub>			$C_{i}$	n		average
									7.63%
Co-kriging	1.74%	0.72%	0.48%	0.60%	27.87%	9.85%	6.92%	8.31%	7.06%(-7.4%)
MFNN-ROM	1.73%	1.09%	0.54%	0.31%	6.36%	5.87%	3.62%	2.59%	2.76%(-63.8%)

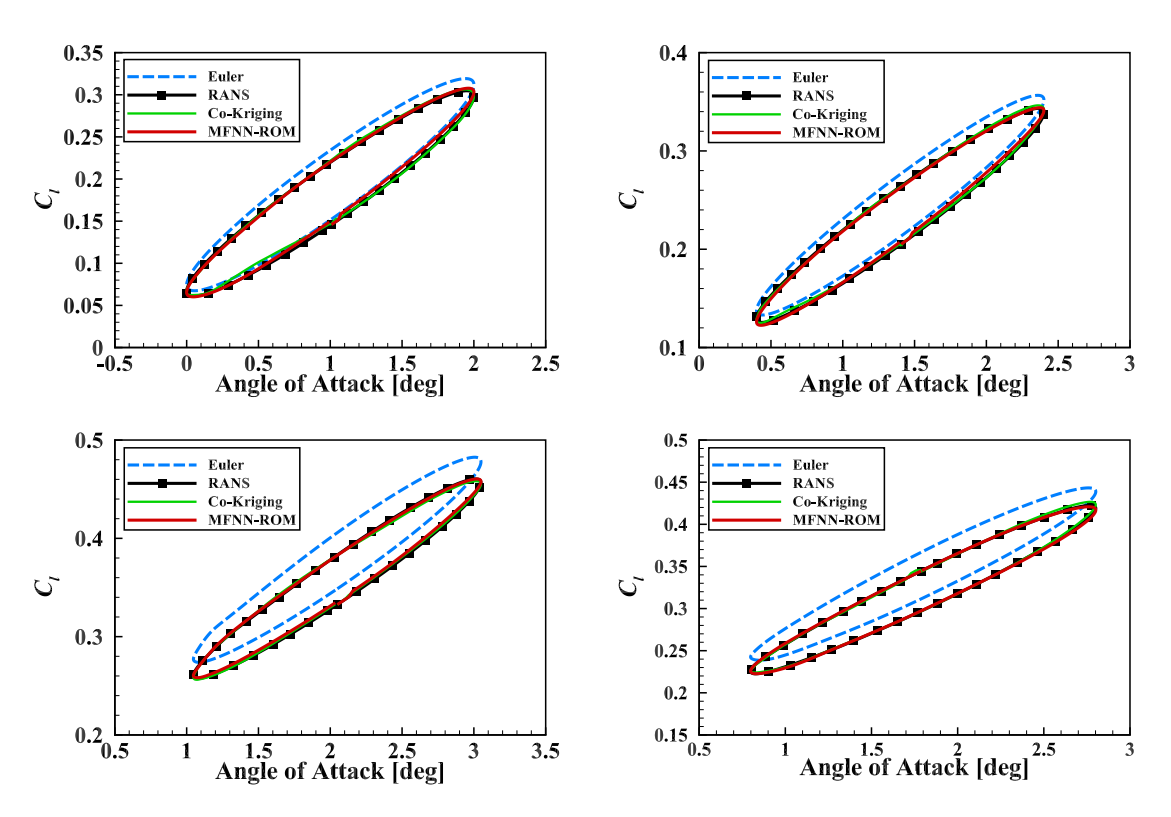


Figure 9 – Prediction results of lift coefficients across multiple Mach numbers

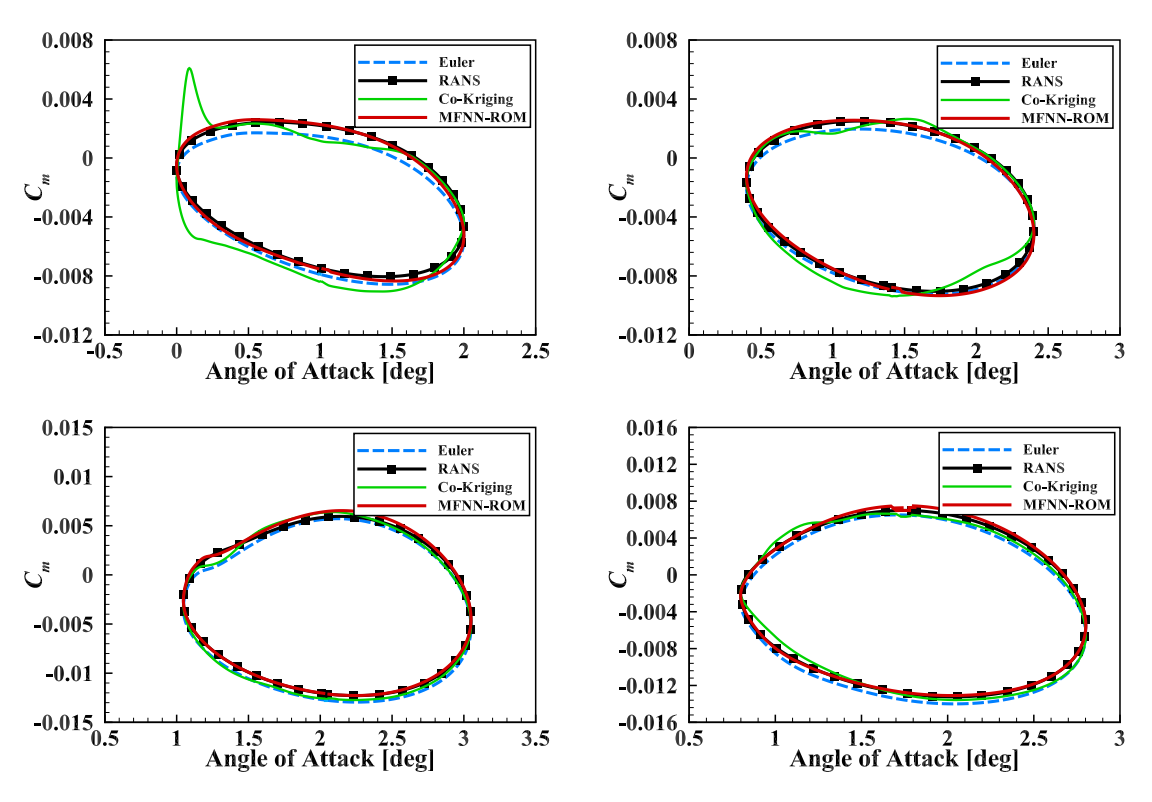


Figure 10 – Prediction results of moment coefficients across multiple Mach numbers

## 4. Flutter Predictions and Discussion

The above unsteady aerodynamic cases verified the effectiveness of the proposed MF aerodynamic modeling method. Next, based on two-degree-of-freedom aeroelastic simulations, the model's generalization capabilities will be further validated and discussed.

# 4.1 Training of MFNN-ROM

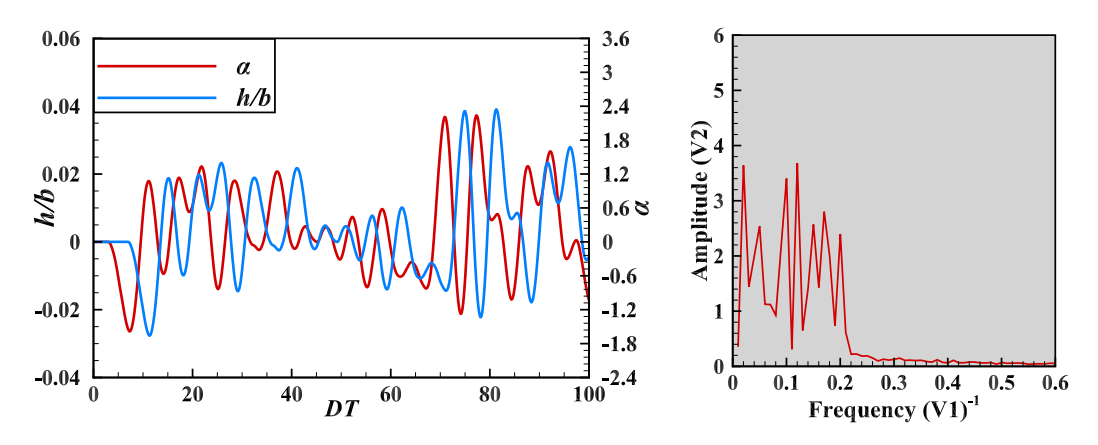


Figure 11 – Random signals of unsteady motions

As shown in Fig. 6, the training data of the MFNN-ROM needed to be obtained through the simulation of unsteady forced motions. To fully cover the frequencies and angles of attack during unsteady pitching and plunging motion, motions controlled by random signals were selected for model training. The time histories of the angles of attack and plunging displacements are shown in Fig. 11. The reduced frequency of the unsteady motions covered the range of 0–0.2. DT = 0.1 in the calculation process. Each set of training data contained 1000 sample points. The training cases were calculated at Mach numbers of 0.7 and 0.75 with  $\alpha_0$  values of 1 and 2 deg. During the training of these four sets of data, the MFNN-ROM needed to have a generalization capability across multiple Mach numbers, angles of attack, and dimensionless velocities to make flutter predictions.

## 4.2 Online flutter predictions by MFNN-ROM

Based on the MFNN-ROM, flutter simulations were conducted for flow conditions with Mach numbers ranging from 0.6 to 0.75 and dimensionless velocities ranging from 0.2 to 1.0. The comparisons of the simulation results for different Mach numbers and angles of attack at different  $v^*$  are shown in Fig. 12-15. Due to the differences in the solver accuracies, there were significant differences between the two coupled simulation results. At Mach numbers 0.65 and 0.7, the RANS calculation results indicated that the current dimensionless velocity was in the critical state of flutter. This was not consistent with the Euler simulation results. The proposed MFNN model accurately realized the data correction of the coupling process through online prediction. The above prediction results showed that the proposed model achieved accurate predictions, whether it was a convergence process, a critical process, or a divergence process. It is worth noting that the prediction results at Mach numbers from 0.6 to 0.7 could be extrapolated for other Mach numbers. This was also because the Euler results possessed a certain degree of accuracy that reflected the Mach number effect on the unsteady aerodynamic forces. Based on the online prediction, the MFNN-ROM method can achieve better generalization performance than offline data-driven modeling.

The results show that the transition of the coupled system from the divergence state to the critical state can be achieved even with model corrections halfway through the Euler simulation. Due to its ability to generalize to the initial states, the proposed model has a greater application potential than offline models.

It can be found that the flutter boundaries solved by the Euler method differed significantly from those of the RANS method. The average error between the HF and LF predictions reached 0.119. By contrast, the average error in the prediction results of the MF model was 0.025. To obtain predictions

for the flutter boundaries, simulations of the dimensionless velocities corresponding to each flow state are required. Dimensionless velocities were taken at 0.05 intervals. Therefore, a total of 204 states  $(17 \times 4 \times 3)$  needed to be calculated. A comparison of the simulation times required by the three different methods is given in Table 3. The online prediction time of the MFNN-ROM was essentially the same as that of the LF method, with the main computational cost increase in the offline phase of data generation and training. The MF method still offered significant efficiency advantages over the HF simulations. Compared with LF methods, the MF method achieved a significant increase in accuracy with only a small increase in the total cost.

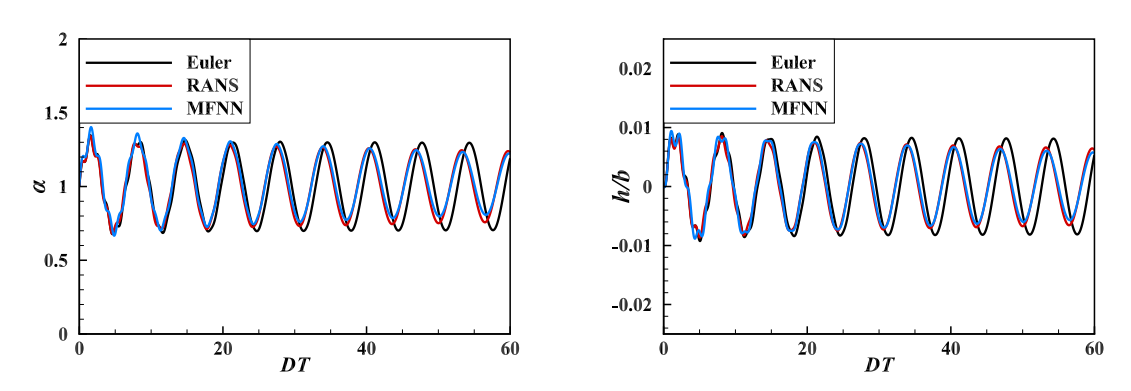


Figure 12 – Flutter predictions at Ma = 0.60,  $\alpha_0 = 1.0$  deg, and  $\nu^* = 0.75$ 

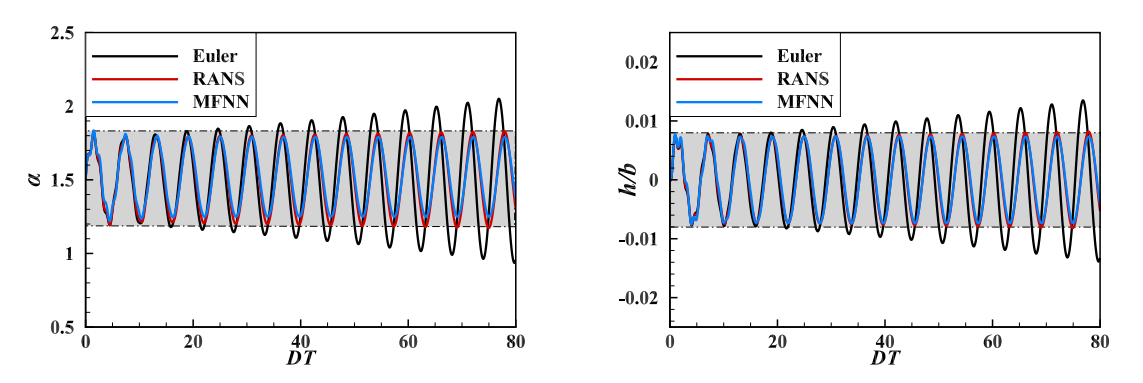


Figure 13 – Flutter predictions at Ma = 0.65,  $\alpha_0 = 1.5$  deg, and  $\nu^* = 0.75$ 

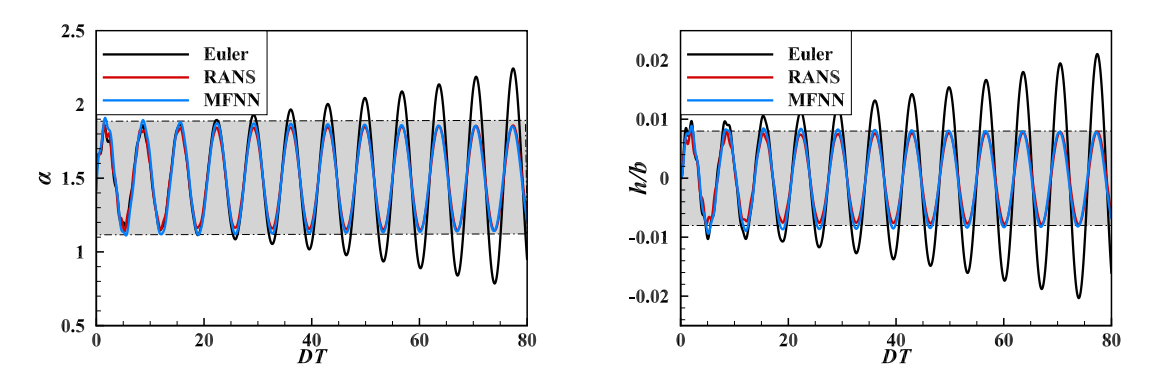
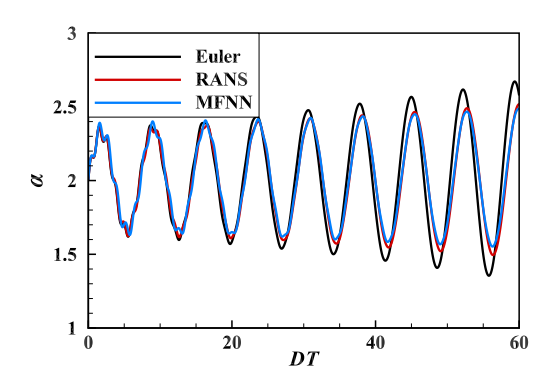


Figure 14 – Flutter predictions at Ma = 0.70,  $\alpha_0$  = 1.5 deg, and  $\nu^*$  =0.60

## 5. Conclusion

In the present work, an efficient ROM method based on an MF modeling framework for transonic flutter prediction was proposed. Using a data-driven approach, the proposed model bridges the



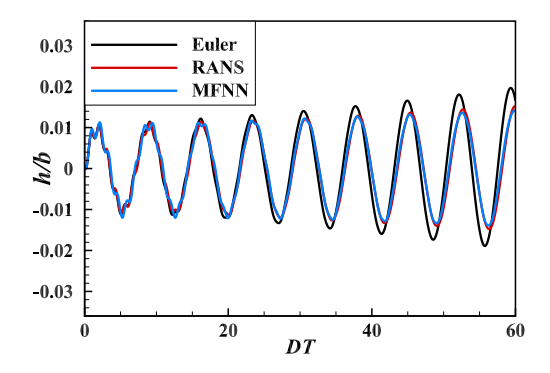


Figure 15 – Flutter predictions at Ma = 0.75,  $\alpha_0$  = 2.0 deg, and  $\nu^*$  = 0.60

Table 3 – Comparison of computation times for flutter boundary predictions

	Calculation cases	Total time		
Euler	204 LF cases	about 816 h (204 × 4)		
RANS	204 HF cases	about 3264 h (204 × 16)		
MFNN-ROM	4 HF cases + 208 LF cases	about 896.5 h (offline phase 80.5 h + online phase 816 h)		

gap between the accuracy and efficiency of LF and HF simulations. Through offline training and online prediction, the proposed MFNN-ROM enables aerodynamic and aeroelastic predictions across multiple Mach numbers. The proposed method was validated by modeling of the transonic aeroelastic simulation of the NACA64A010 airfoil. The results showed that the proposed method provides an online correction approach to improve the accuracy and generalization of the coupled simulation. Compared with the traditional ROM methods for predictions of nonlinear aeroelasticity, the proposed method has the following three characteristics.

- 1. The inputs to the MFNN model include both outputs of the LF solver, which allows the construction of the neural network model to take into account the differences in the inputs. With the proposed neural network architecture, the aerodynamic prediction accuracy of this method was better than that of the co-kriging method.
- 2. The aeroelastic MFNN-ROM does not completely replace the CFD/CSD time-domain simulation but rather achieves aerodynamic correction of the LF simulation by a data-driven model through online prediction. This significantly reduces the data requirements in the offline phase and improves the generalization of the data-driven simulation.
- 3. The prediction results for the transonic flutter show that the MF method could significantly improve the prediction accuracy by more than four times at no more than a 10% additional computational cost. This improvement will be more significant in wind tunnel tests.

This work provides a viable solution for MF online aerodynamic modeling correction and coupling simulations. Future work will consider the use of this approach for flight simulations to carry out flight control with digital twins.

## 6. Contact Author Email Address

The corresponding author email address is aeroelastic@nwpu.edu.cn (Weiwei Zhang).

# 7. Copyright Statement

The authors confirm that they, and/or their company or organization, hold copyright on all of the original material included in this paper. The authors also confirm that they have obtained permission, from the copyright holder of any third party material included in this paper, to publish it as part of their paper. The authors confirm that they give permission, or have obtained permission from the copyright holder of this paper, for the publication and distribution of this paper as part of the ICAS proceedings or as individual off-prints from the proceedings.

## References

- [1] Max MJ Opgenoord, Mark Drela, and Karen E Willcox. Physics-based low-order model for transonic flutter prediction. *AIAA Journal*, 56(4):1519–1531, 2018.
- [2] Andrew Thelen, Leifur Leifsson, and Philip Beran. Aeroelastic flutter prediction using multifidelity modeling of the generalized aerodynamic influence coefficients. *AIAA Journal*, 58(11):4764–4780, 2020.
- [3] Jieyun Pan and Feng Liu. Wing flutter prediction by a small-disturbance euler method on body-fitted curvilinear grids. *AIAA Journal*, 57(11):4873–4884, 2019.
- [4] Earl H Dowell and Kenneth C Hall. Modeling of fluid-structure interaction. *Annual Review of Fluid Mechanics*, 33(1):445–490, 2001.
- [5] Marco Casoni and Ernesto Benini. A review of computational methods and reduced order models for flutter prediction in turbomachinery. *Aerospace*, 8(9):242, 2021.
- [6] Xu Wang, Jiaqing Kou, and Weiwei Zhang. A new dynamic stall prediction framework based on symbiosis of experimental and simulation data. *Physics of Fluids*, 33(12):127119, 2021.
- [7] Rui Huang, Haojie Liu, Zhijun Yang, Yonghui Zhao, and Haiyan Hu. Nonlinear reduced-order models for transonic aeroelastic and aeroservoelastic problems. *AIAA Journal*, 56(9):3718–3731, 2018.
- [8] Steven L Brunton, J Nathan Kutz, Krithika Manohar, Aleksandr Y Aravkin, Kristi Morgansen, Jennifer Klemisch, Nicholas Goebel, James Buttrick, Jeffrey Poskin, Adriana W Blom-Schieber, et al. Data-driven aerospace engineering: reframing the industry with machine learning. *AIAA Journal*, 59(8):2820–2847, 2021.
- [9] Weiwei Zhang, Jiaqing Kou, and Ziyi Wang. Nonlinear aerodynamic reduced-order model for limit-cycle oscillation and flutter. *AIAA Journal*, 54(10):3304–3311, 2016.
- [10] Pengyin Liu, Guohua Yu, Xiaocheng Zhu, and Zhaohui Du. Unsteady aerodynamic prediction for dynamic stall of wind turbine airfoils with the reduced order modeling. *Renewable Energy*, 69:402–409, 2014.
- [11] Haojie Liu, Haiyan Hu, Yonghui Zhao, and Rui Huang. Efficient reduced-order modeling of unsteady aerodynamics robust to flight parameter variations. *Journal of Fluids and Structures*, 49:728–741, 2014.
- [12] Michael Candon, Robert Carrese, Hideaki Ogawa, and Pier Marzocca. Identification of freeplay and aero-dynamic nonlinearities in a 2d aerofoil system with via higher-order spectra. *The Aeronautical Journal*, 121(1244):1530–1560, 2017.
- [13] Zhiqiang Chen, Yonghui Zhao, and Rui Huang. Parametric reduced-order modeling of unsteady aerodynamics for hypersonic vehicles. *Aerospace Science and Technology*, 87:1–14, 2019.
- [14] Cameron Brown, Greg McGowan, Kilian Cooley, Joe Deese, Tim Josey, Earl H Dowell, and Jeffrey P Thomas. Convolution/volterra reduced-order modeling for nonlinear aeroelastic limit cycle oscillation analysis and control. *AIAA Journal*, 60(12):6647–6664, 2022.
- [15] Jiaqing Kou and Weiwei Zhang. Data-driven modeling for unsteady aerodynamics and aeroelasticity. *Progress in Aerospace Sciences*, 125:100725, 2021.
- [16] Rebecca Zahn, Maximilian Winter, Moritz Zieher, and Christian Breitsamter. Application of a long short-term memory neural network for modeling transonic buffet aerodynamics. *Aerospace Science and Technology*, 113:106652, 2021.
- [17] Xu Wang, Jiaqing Kou, and Weiwei Zhang. Unsteady aerodynamic modeling based on fuzzy scalar radial basis function neural networks. *Proceedings of the Institution of Mechanical Engineers, Part G: Journal of Aerospace Engineering*, 233(14):5107–5121, 2019.
- [18] Kai Li, Jiaqing Kou, and Weiwei Zhang. Deep neural network for unsteady aerodynamic and aeroelastic modeling across multiple mach numbers. *Nonlinear Dynamics*, 96:2157–2177, 2019.
- [19] Maximilian Winter and Christian Breitsamter. Neurofuzzy-model-based unsteady aerodynamic computations across varying freestream conditions. *AIAA Journal*, 54(9):2705–2720, 2016.
- [20] Alexandre N Marques, Max MJ Opgenoord, Remi R Lam, Anirban Chaudhuri, and Karen E Willcox. Multifidelity method for locating aeroelastic flutter boundaries. *AIAA Journal*, 58(4):1772–1784, 2020.
- [21] Xu Wang, Jiaqing Kou, and Weiwei Zhang. Multi-fidelity surrogate reduced-order modeling of steady flow estimation. *International Journal for Numerical Methods in Fluids*, 92(12):1826–1844, 2020.
- [22] Orazio Pinti, Assad A Oberai, Richard Healy, Robert J Niemiec, and Farhan Gandhi. Multi-fidelity approach to predicting multi-rotor aerodynamic interactions. AIAA Journal, 60(6):3894–3908, 2022.
- [23] Benjamin Peherstorfer and Karen Willcox. Dynamic data-driven reduced-order models. *Computer Methods in Applied Mechanics and Engineering*, 291:21–41, 2015.
- [24] M Giselle Fernández-Godino, Chanyoung Park, Nam H Kim, and Raphael T Haftka. Issues in deciding whether to use multifidelity surrogates. *AIAA Journal*, 57(5):2039–2054, 2019.
- [25] Xuhui Meng and George Em Karniadakis. A composite neural network that learns from multi-fidelity

- data: Application to function approximation and inverse pde problems. *Journal of Computational Physics*, 401:109020, 2020.
- [26] Markus P Rumpfkeil and Philip Beran. Multi-fidelity surrogate models for flutter database generation. *Computers & Fluids*, 197:104372, 2020.
- [27] Zhong-Hua Han, Zimmermann, and Stefan Görtz. Alternative cokriging method for variable-fidelity surrogate modeling. *AIAA Journal*, 50(5):1205–1210, 2012.
- [28] Halil Kaya, Hakan Tiftikçi, Ümit Kutluay, and Evren Sakarya. Generation of surrogate-based aerodynamic model of an ucav configuration using an adaptive co-kriging method. Aerospace Science and Technology, 95:105511, 2019.
- [29] Jiaqing Kou and Weiwei Zhang. Multi-fidelity modeling framework for nonlinear unsteady aerodynamics of airfoils. *Applied Mathematical Modelling*, 76:832–855, 2019.
- [30] Haolin Liu, Chuanqiang Gao, Xu Wang, Zihao Dou, and Weiwei Zhang. Aeroelastic prediction in transonic buffeting flow with data fusion method. *Aerospace Science and Technology*, page 108097, 2023.
- [31] Philippe Spalart and Steven Allmaras. A one-equation turbulence model for aerodynamic flows. In *30th aerospace sciences meeting and exhibit*, page 439, 1992.
- [32] Aukje De Boer, Martijn S Van der Schoot, and Hester Bijl. Mesh deformation based on radial basis function interpolation. *Computers & Structures*, 85(11-14):784–795, 2007.
- [33] Sanford S Davis. Naca 64a010 (nasa ames model) oscillatory pitching. AGARD report, 702:1982, 1982.
- [34] Weiwei Zhang and Zhengyin Ye. Reduced-order-model-based flutter analysis at high angle of attack. *Journal of Aircraft*, 44(6):2086–2089, 2007.
- [35] S Chen, SA Billings, CFN Cowan, and PM Grant. Non-linear systems identification using radial basis functions. *International Journal of Systems Science*, 21(12):2513–2539, 1990.
- [36] Russell Eberhart and James Kennedy. A new optimizer using particle swarm theory. In MHS'95. Proceedings of the Sixth International Symposium on Micro Machine and Human Science, pages 39–43. leee, 1995.
- [37] Xuhao Peng, Jiaqing Kou, and Weiwei Zhang. Multi-fidelity nonlinear unsteady aerodynamic modeling and uncertainty estimation based on hierarchical kriging. *Applied Mathematical Modelling*, 122:1–21, 2023.